Physica E 129 (2021) 114601

Contents lists available at ScienceDirect

Physica E: Low-dimensional Systems and Nanostructures

journal homepage: http://www.elsevier.com/locate/physe

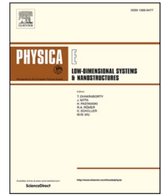

Influence of piezoelectric phonons on the magneto optical transition linewidth in GaN and GaAs

Le Thi Quynh Huong [a,b], Le Ngoc Minh [c], Luong Thi Huong [d], Nguyen Dinh Hien [e,f,*]

[a] *Institute of Research and Development, Duy Tan University, Danang, 550000, Viet Nam*
[b] *Faculty of Natural Sciences, Duy Tan University, Danang, 550000, Viet Nam*
[c] *Faculty of Physics, University of Sciences, Hue University, Hue City, Viet Nam*
[d] *Nha Trang National Ethnic Minority Pre-university, Nha Trang City, Khanh Hoa Province, Viet Nam*
[e] *Laboratory of Magnetism and Magnetic Materials, Advanced Institute of Materials Science, Ton Duc Thang University, Ho Chi Minh City, Viet Nam*
[f] *Faculty of Applied Sciences, Ton Duc Thang University, Ho Chi Minh City, Viet Nam*

A R T I C L E I N F O

Keywords:
Piezoelectric phonon
GaN and GaAs
MOTLWs

A B S T R A C T

We compare piezoelectric phonon scattering mechanism with optical phonon one in both Gallium arsenide (GaAs) and Gallium nitride (GaN) materials of a quantum well through the their contribution to the magneto-optical transition linewidths (MOTLWs). Applying the projection-operator and the profile methods to compute the magneto-optical conductivity tensor (MOCT), magneto-optical absorption power (MOAP), and MOTLWs. Numerical calculation results show that the MOTLWs increase as the temperatures and the magnetic fields increase, but decrease as the electron density and the well width increase for both GaN and GaAs materials. In particular, the MOTLWs due to piezoelectric phonons vary sharper and have larger value than they do due to optical phonons in both GaN and GaAs materials, and the MOTLWs of GaN are larger than those of GaAs for both piezoelectric and optical phonon scattering mechanisms. As small enough quantum-well-width, the piezoelectric phonon modes play an important role and they should be considered in studying the magneto optical transition properties in low-dimensional electron systems.

1. Introduction

The investigation of the magneto-optical transition properties for low dimensional electrons systems is known to be a useful tool for studying the electronic-structure of solid, this is due to absorption linewidths are known to be very sensitive to the type of mechanisms of scattering influencing the transport-behavior of electrons in semiconductor structures [1–6]. In recent years, semiconductor materials possess wide-band-gaps, for instance GaN and ZnO have attracted much interest for device applications such as the optoelectronic and electronic devices. Where GaN and ZnO have band-gaps of E_g respectively are 3.44 eV and 3.37 eV [7]. Continuing progress of GaN-material-based optoelectronic-devices for conspicuous device applications has created the significant development of the achievement of the laser diodes (LD's) and the commercialization of the high brightness green/blue light-emitting diodes (LED's) [8–10]. In addition to potential applications of GaN material in fabrication of optoelectronic devices, GaN is also fairly interesting from one purely physical-viewpoint. The fundamental physical natures of the GaN material can be strongly influenced and even defined by the anisotropy of the crystal quantum structures and the spatial-quantization of the states of the carrier [8]. The study of electron–phonon scattering mechanism in low-dimensional electron systems has not only practical-significance or great-importance for device applications but also important theoretical meaning in the semiconductor physics. The characteristics of quantum well systems are defined mostly through electron scattering with phonon in semiconductor physics near the room temperature. Therefore, to better understand the physical properties of electrons system in GaN and GaAs wells, the study of electron–phonon scattering mechanism is the most effective way. It is known that the type of interactions such as electron–impurity, electron–electron, and electron–phonon interactions are known to be main scattering mechanisms in low-dimensional systems. Among them electron–phonon scattering mechanism is dominant, since as low electron density as that in ordinary semiconductors, at the same time temperature of electrons system also is low then electron interaction with electron and impurity can be neglected in this case [4]. There are many types

* Corresponding author. Laboratory of Magnetism and Magnetic Materials, Advanced Institute of Materials Science, Ton Duc Thang University, Ho Chi Minh City, Viet Nam.
E-mail addresses: letquynhhuong1@duytan.edu.vn (L.T.Q. Huong), nguyendinhhien@tdtu.edu.vn (N.D. Hien).

https://doi.org/10.1016/j.physe.2020.114601
Received 29 October 2020; Received in revised form 21 November 2020; Accepted 23 December 2020
Available online 21 January 2021
1386-9477/© 2021 Elsevier B.V. All rights reserved.

of phonon modes for interactions with electron such as piezoelectric phonon, deformation phonon, optical phonon [11], acoustic phonon [12], interface phonon [13], confine phonon [14–17], etc. However, in this paper we are interested in the first one, and compared with the third one. The electron–piezoelectric phonon interactions occur in crystal lacking an inversion symmetry, for instance wurtzite structures or semiconductors with sphalerite. The electrons–piezoelectric phonons interactions due to a macroscopic polarization is produced from the application of an external-strain to piezoelectric material [4]. There are many theoretical approaches to study the deformation, acoustic, and optical phonon scattering mechanisms [12,18–21] while electron–piezoelectric phonon scattering mechanism has been less interested to study in low-dimensional systems. Moreover, excellent acousto-electric properties only have in piezoelectric crystals. Therefore, such piezoelectric materials as GaN and GaAs they can be used for diverse applications such as amplifiers for ultrasonic wave, fluorescent pigments, and actinometers ect. Besides, the calculations of Jun-jie Shi [8] showed that electrophonon scatterings vigorously effected on the optical property as well as transport property of GaN semiconductors. Obviously, it is very imperative and necessary to investigate the contribution of piezoelectric phonons to electrophonon interactions in group-III nitride semiconductor structures in general and in GaN in particular. The investigation of the magneto-optical transition linewidths is known as a useful tool to examine the transport-behavior of electron system in quantum wells [1–4]. There are many theoretical models to consider the quantum transition properties in different methodologies, among them we utilize the projection operator method because projection operators are define explicitly which can give an explicit magneto-optical transitions formula. On the other hand, the resolvent quantity contained in the MOCT being expanded with help of projection operators, and using this method we can obtaine the different Lorentzian line formula. The aim of this work is to consider the effects of piezoelectric phonons on the MOTLWs in comparison with optical phonon in both GaN and GaAs. First, we present the theory for electrons scattering mechanisms with piezoelectric and optical phonons in both GaN and GaAs materials of quantum wells. Next, we will calculate analytically the MOAP caused by piezoelectric phonon and optical phonon in both GaN and GaAs wells based on the projection operator. Finally, we show numerical calculated results for magneto-optical transition linewidth caused by the piezoelectric phonon scattering in comparison with that due to the optical phonons scattering in both GaN and GaAs by using profile method, and they are discussed in detail.

2. Scattering mechanisms of piezoelectric and optical phonons in both GaN and GaAs materials of quantum wells

We consider optical and piezoelectric phonon scattering mechanisms in GaN and GaAs wells, in the presence of magnetic field **B**, with confining potential $V(z)$ for electrons system in well structure is given as

$$V(z) = \begin{cases} 0, & |z| < L_z/2, \\ \infty, & |z| > L_z/2, \end{cases} \tag{1}$$

the eigenfunctions $\Phi(\mathbf{r})$ can be written as [22]

$$\Phi(\mathbf{r}) = \frac{1}{\sqrt{L_y}}\Psi_N(x - x_0)\exp(ik_y y)\psi_n(z), \tag{2}$$

where the harmonic oscillator function and cyclotron radius respectively are symbolled by $\Psi_N(x - x_0)$ and $a_c = \sqrt{\hbar c/(eB)}$, here $x_0 = -a_c^2 k_y$. Moreover, we let the specimen dimension be L_y and wave vector along the y-axis be k_y. The corresponding eigenfunction, $\psi_n(z)$, is described by [22]

$$\psi_n(z) = \left(\frac{2}{L_z}\right)^{1/2}\sin\left(\frac{n\pi z}{L_z} + \frac{n\pi}{2}\right), \tag{3}$$

and the corresponding energy eigenvalue $E(nN)$ is

$$E(Nn) = \left(N + \frac{1}{2}\right)\hbar\omega_c + n^2\varepsilon_0, \tag{4}$$

where N and n respectively are the Landau and electrical-subband level numbers. The cyclotron-resonance frequency and lowest electrical subband energy respectively are symbolled by $\omega_c = eB/m^*$ and $\varepsilon_0 = \hbar^2\pi^2/(2\,m^* L_z^2)$, in which m^* and L_z respectively are the effective mass and well-width.

Piezoelectric and optical phonon scattering mechanisms with matrix element is given as [23–28]

$$|\langle i|H_{e-ph}|f\rangle|^2 = |V_q|^2|M_{nn'}(q_z)|^2|J_{NN'}(u)|^2\delta_{k_\perp^f, k_\perp^i \pm q_\perp}, \tag{5}$$

where we let the overlap integral over dz be $M_{nn'}(q_z)$, and it is given as below

$$M_{nn'}(q_z) = \int_{-L_z/2}^{L_z/2}\psi_n(z)\exp(iq_z z)\psi_{n'}(z)dz, \tag{6}$$

the quantity, $J_{NN'}(u)$, in Eq. (5) is related to the Laguerre polynomial, $L_{n2}^{n1-n2}(u)$, and defined as

$$|J_{NN'}(u)|^2 = \frac{n_2! e^{-u}u^{n1-n2}}{n_1!}[L_{n2}^{n1-n2}(u)]^2, \tag{7}$$

here $n1 = max\{N, N'\}, u = q_\perp^2 a_c^2/2, n2 = min\{N, N'\}$. Also, the coupling coefficient, V_q, in Eq. (5) is the quantity depends on the type of phonons:

2.1. Piezoelectric phonon scattering mechanism

The coupling coefficient V_q in Eq. (5) for electron–piezoelectric-phonon scattering mechanism is written by [4]

$$|V_q|^2 = \frac{\kappa^2\hbar e^2 s}{2\Omega\epsilon_s\epsilon_0}\frac{q^3}{(q^2 + q_d^2)^2}, \tag{8}$$

where κ, Ω, and s respectively refer to the electromechanical (piezoelectric) coupling constant, the volume of the quantum well electrons system, and the speed of sound. ϵ_s and ϵ_0 are the static-dielectric and vacuum-dielectric constants. The factor $q_d^2 = n_e e^2/\epsilon_s\epsilon_0 k_B T$ in Eq. (8) is referred to as the reciprocal of the Debye screening length, where we let the uniform electron concentration be n_e.

As we know, the electromechanical coupling, κ, has a complex dependence. For wurtzite kind lattice such as GaN, the piezoelectric coupling constant κ is replaced by $\bar{\kappa}$ in the isotropic model, and it is determined by [29]

$$\overline{\kappa^2} = \frac{1}{\nu\epsilon_0\rho}\left(\frac{\langle e_L^2\rangle}{s_L^2} + \frac{\langle e_T^2\rangle}{s_T^2}\right), \tag{9}$$

where $\bar{\kappa}$ is the average value of κ, the transverse and longitudinal sound speed are given by

$$s_T = \sqrt{\frac{c_T}{\rho}}, s_L = \sqrt{\frac{c_L}{\rho}}, \tag{10}$$

with c_T and c_L refer to the spherical elastic constant for the transverse and longitudinal waves, respectively, and they have the equations as follows:

$$c_L = c_{12} + 2c_{44} + \frac{3c^*}{5}, c_T = c_{44} + \frac{c^*}{5}, \tag{11}$$

here the factor c^* being the measurement of elastic anisotropy, and $c^* = 0$ in the isotropic crystals case, c^* is written by

$$c^* = c_{11} - c_{12} - 2c_{44}, \tag{12}$$

and ρ denotes the density of mass. On the other hand, the factor $\langle e_T^2\rangle$ in Eq. (9) for the transverse waves be expressed as

$$\langle e_T^2\rangle = \frac{2}{35}(e_{33}-e_{31}-e_{15})^2 + \frac{16}{105}e_{15}(e_{33}-e_{31}-e_{15}) + \frac{16}{35}e_{15}^2, \quad (13)$$

and the factor $\langle e_L^2\rangle$ for the longitudinal waves is

$$\langle e_L^2\rangle = \frac{e_{33}^2}{7} + \frac{4e_{33}(e_{31}+2e_{15})}{35} + \frac{8e_{31}^2}{35}, \quad (14)$$

where we let the reduced-notation of the $e_{ik\ell}$-component of the piezoelectric constant tensor e be e_{ij}.

For sphalerite type lattice, for instance ZnS, GaAs etc., the piezoelectric coupling constant $\bar{\kappa}$ is defined by [30]

$$\overline{\kappa^2} = \frac{12e_{14}^2}{35\nu\epsilon_0\rho}\left(\frac{1}{s_L^2}+\frac{1}{s_T^2}\right), \quad (15)$$

noting that the contribution of the other components vanish and where $e_{14} = e_{25} = e_{36}$.

2.2. Optical phonon scattering mechanism

The coupling coefficient, V_q, for electron–optical-phonon scattering mechanism is given by

$$|V_q|^2 = \frac{e^2\hbar\omega_0}{2\Omega\epsilon_0}\left(\frac{1}{\epsilon_\infty}-\frac{1}{\epsilon_s}\right)\frac{q^2}{(q^2+q_d^2)^2}, \quad (16)$$

where $\hbar\omega_0$ and ϵ_∞ refer to the LO-phonon energy and the optical dielectric constant, respectively.

3. Analytical calculation of the MOAP caused by piezoelectric and optical phonon scatterings in both GaN and GaAs quantum wells

3.1. MOCT caused by the piezoelectric- and optical-phonon scatterings

Under the influence of the an electromagnetic field (EMF) where the EMF frequency ω polarized circularly in the plane (x, y), the electrons system in quantum wells structure have the MOCT is determined as [31, 32]

$$\Theta_\pm(\omega) = \frac{i}{\omega}\lim_{b\to0^+}\sum_\gamma (j_\gamma^+)^* T_R\{\rho(H)[Y, c_\gamma^\dagger c_{\gamma+1}]\}, \quad (17)$$

here the annihilation (creation) and Liouville operators are symbolled by c_γ ($c_\gamma^\dagger$) and L. The density operator is $\rho(H)$, the matrix element of the current is obtained from the eigenstate as $j_\gamma^+ = -ie\sqrt{2\hbar\omega_c(N_\gamma+1)/m^*}$. The factor Y is defined by $Y = (\hbar\overline{\omega} - L)^{-1}J_+$ where $J_+ = J_x + iJ_y$ is referred to as the current density operator. $\overline{\omega} = \omega - ib$, $(b \to 0^+)$. The EMF frequency and many body trace are symbolled by ω and T_R, respectively. In this paper the projection operators

$$P_\gamma Y = \frac{\langle Z\rangle_\gamma}{\langle J_+\rangle_\gamma}J_+, Q_\gamma = 1 - P_\gamma, \quad (18)$$

are used to calculate the MOCT and the MOAP. Where the factor $\langle Z\rangle_\gamma$ in Eq. (18) is defined as follows

$$\langle Z\rangle_\gamma = T_R\{\rho(H)[Z, b_\gamma^\dagger b_{\gamma+1}]\}. \quad (19)$$

The operator $Q_\gamma = 1 - P_\gamma$ is used to apply on the right hand side of the Liouville operator, namely $L = L(Q_\gamma + P_\gamma)$, along with the help of the (AB) identity is defined by the following equation

$$(A-B)^{-1} = A^{-1} + A^{-1}B(A-B)^{-1}, \quad (20)$$

and using the quantity, $\langle J_+\rangle_\gamma = j_\gamma^+(f_{\gamma+1} - f_\gamma)$, we obtain the equation of the MOCT as below

$$\Theta_\pm(\omega) = \frac{i}{\omega}\lim_{b\to0^+}\sum_\gamma \frac{|j_\gamma^+|^2(f_{\gamma+1}-f_\gamma)}{\hbar\overline{\omega} - \hbar\omega_c - \hbar\lambda_\gamma(\overline{\omega})}, \quad (21)$$

in which we let the Fermi distribution function be f_γ, and $\lambda_\gamma(\overline{\omega})$ is referred to as the linewidth function determined by

$$\begin{aligned}(f_{\gamma+1}-f_\gamma)\quad \hbar\lambda_\gamma(\overline{\omega}) = \\ \sum_{\vec{q},\tau}|C_{\gamma\tau}(\vec{q})|^2\Bigg[\frac{(1+N_{\vec{q}})f_{\gamma+1}(1-f_\tau) - N_{\vec{q}}f_\tau(1-f_{\gamma+1})}{\hbar\overline{\omega}+\hbar\omega_{\vec{q}} - E_{\gamma+1,\tau}} \\ + \frac{N_{\vec{q}}f_{\gamma+1}(1-f_\tau) - (1+N_{\vec{q}})f_\tau(1-f_{\gamma+1})}{\hbar\overline{\omega}-\hbar\omega_{\vec{q}} - E_{\gamma+1,\tau}}\Bigg] \\ +\sum_{\vec{q},\tau}|C_{\tau,\gamma+1}(\vec{q})|^2\Bigg[\frac{(1+N_{\vec{q}})f_\tau(1-f_\gamma) - N_{\vec{q}}f_\gamma(1-f_\tau)}{\hbar\overline{\omega}+\hbar\omega_{\vec{q}} - E_{\tau\gamma}} \\ + \frac{N_{\vec{q}}f_\tau(1-f_\gamma) - (1+N_{\vec{q}})f_\gamma(1-f_\tau)}{\hbar\overline{\omega}-\hbar\omega_{\vec{q}} - E_{\tau\gamma}}\Bigg]\end{aligned} \quad (22)$$

3.2. MOAP caused by piezoelectric- and optical-phonon scatterings

The average MOAP, $MOAP(\omega)$, per unit volume of electrons system in quantum well caused by the piezoelectric- and optical-phonon scatterings delivered by an EMF with amplitude E_0 is given as [31]

$$MOAP(\omega) = \frac{E_0^2}{2}\mathrm{Re}\{\Theta_\pm(\omega)\}, \quad (23)$$

where the real part of the MOCT in Eq. (21) is symbolled by $\mathrm{Re}\{\Theta_\pm(\omega)\}$.

To obtain the explicit equation for the $MOAP(\omega)$ we have to calculate the real-part, $\mathrm{Re}\{\Theta_\pm(\omega)\}$, in detail as follows. We can see that the quantity $\lambda_\gamma(\overline{\omega})$ in expression (21) which is determined in expression (22) be a complex-function. Hence it can be again written as

$$\lambda_\gamma(\overline{\omega}) = \zeta_\gamma(\omega) + i\chi_\gamma(\omega), \quad (24)$$

here we let the imaginary and real parts be $\chi_\gamma(\omega)$ and $\zeta_\gamma(\omega)$, where they are related to the spectrum linewidth and the peak shift, respectively. However, in the extreme quantum limit, the quantity $\zeta_\gamma(\omega)$ can be neglected in comparison to the quantity ω_c. We apply the Dirac identity which is presented as below

$$\lim_{\Delta\to0^+}\frac{1}{(z-i\Delta)} = P\left(\frac{1}{z}\right) + i\pi\delta(z), \quad (25)$$

then the spectrum linewidth function, $\chi_\gamma(\omega)$, is obtained as follows

$$\begin{aligned}(f_{\gamma+1}-f_\gamma)\hbar\chi_\gamma(\omega) = \\ \pi\sum_{\tau,\vec{q}}|C_{\gamma,\tau}(\vec{q})|^2\{[(1+N_{\vec{q}})f_{\gamma+1}(1-f_\tau) - N_{\vec{q}}f_\tau(1-f_{\gamma+1})]\delta(\varepsilon_1^+) \\ + [N_{\vec{q}}f_{\gamma+1}(1-f_\tau) - (1+N_{\vec{q}})f_\tau(1-f_{\gamma+1})]\delta(\varepsilon_1^-)\} \\ +\pi\sum_{\tau,\vec{q}}|C_{\gamma+1,\tau}(\vec{q})|^2\{[(1+N_{\vec{q}})f_\tau(1-f_\gamma) - N_{\vec{q}}f_\gamma(1-f_\tau)]\delta(\varepsilon_2^+) \\ + [N_{\vec{q}}f_\tau(1-f_\gamma) - (1+N_{\vec{q}})f_\gamma(1-f_\tau)]\delta(\varepsilon_2^-)\},\end{aligned} \quad (26)$$

where

$$\varepsilon_1^\pm = \hbar\omega \pm \hbar\omega_{\mathbf{q}} - E_{\gamma+1,\tau}, \quad (27)$$

$$\varepsilon_2^\pm = \hbar\omega \pm \hbar\omega_{\mathbf{q}} - E_{\tau\gamma}. \quad (28)$$

Inserting $\lambda_\gamma(\varpi)$ from expression (24) into the MOCT, $\Theta_\pm(\omega)$, in Eq. (21), we have

$$\Theta_\pm(\omega)=\frac{i}{\omega}\lim_{b\to 0^+}\sum_\gamma\frac{|j_\gamma^+|^2(f_{\gamma+1}-f_\gamma)}{\hbar\omega-\hbar\omega_c-\hbar\zeta_\gamma(\omega)-i\hbar[\chi_\gamma(\omega)+b]},\quad(29)$$

making some straightforward calculations of the MOCT from the expression (29), we obtain

$$\Theta_\pm(\omega)=\frac{1}{\omega}\sum_\gamma |j_\gamma^+|^2\frac{\hbar(f_\gamma-f_{\gamma+1})\chi_\gamma(\omega)}{(\hbar\omega-\hbar\omega_c)^2+[\hbar\chi_\gamma(\omega)]^2}+i|j_\gamma^+|^2\frac{(f_{\gamma+1}-f_\gamma)(\hbar\omega-\hbar\omega_c)}{(\hbar\omega-\hbar\omega_c)^2+[\hbar\chi_\gamma(\omega)]^2},\quad(30)$$

then the real part, $\mathrm{Re}\{\Theta_\pm(\omega)\}$, of the MOCT for electrons system in wells structure because of the piezoelectric- and optical-phonon scatterings is obtained as

$$\mathrm{Re}\{\Theta_\pm(\omega)\}=\frac{1}{\hbar\omega}\sum_\gamma\frac{|j_\gamma^+|^2(f_\gamma-f_{\gamma+1})\hbar^2\chi_\gamma(\omega)}{(\hbar\omega-\hbar\omega_c)^2+[\hbar\chi_\beta(\omega)]^2},\quad(31)$$

finally, inserting the quantity $\mathrm{Re}\{\Theta_\pm(\omega)\}$ from Eq. (31) into Eq. (23), then the MOAP of quantum-well electrons system caused by piezoelectric and optical phonon scatterings under the influence of an EMF is obtained as below

$$MOAP(\omega)=\frac{E_0^2}{2\hbar\omega}\sum_\gamma\frac{|j_\gamma^+|^2(f_\gamma-f_{\gamma+1})\hbar^2\chi_\gamma(\omega)}{(\hbar\omega-\hbar\omega_c)^2+[\hbar\chi_\gamma(\omega)]^2}.\quad(32)$$

To obtain the explicit equation for the MOAP, *MOAP*(ω), in Eq. (32), we have to calculate in detail the matrix elements $|C_{\gamma,\tau}(\mathbf{q})|^2$ and $|C_{\gamma+1,\tau}(\mathbf{q})|^2$ in Eq. (26) by utilizing the matrix element for electrons interaction with piezoelectric and optical phonons as shown in Eq. (5) where the factor V_q is given by Eqs. (8) and (16) for each kind of phonon (piezoelectric and optical phonons), and using the following relations

$$\sum_{\mathbf{q}}\cdots\to\frac{L_xL_yL_z}{(2\pi)^2}\int_0^\infty q_\perp dq_\perp\int_{-\infty}^\infty dq_z\cdots,\qquad \sum_\tau\cdots\to\sum_n\sum_N\cdots,\quad(33)$$

we obtain the linewidth functions of magneto-optical transitions, $\chi_\gamma(\omega)$, for piezoelectric and optical phonon scattering mechanisms, as shown in sections 3.2.1 and 3.2.2 below.

3.2.1. For piezoelectric phonon scattering mechanism

In the case of electron–piezoelectric-phonon scattering, the linewidth function for magneto-optical transition $\chi_\gamma(\omega)$ in Eq. (32) is obtained as

$$\begin{aligned}\chi_\gamma(\omega)\equiv\chi_\gamma^P(\omega)=&\frac{\kappa^2e^2k_bT}{8\hbar L_z\epsilon_s\epsilon_0}\sum_{N'}\sum_{n'}\frac{2+\delta_{n,n'}}{(f_{N+1,n}-f_{N,n})}\int_0^\infty dq_\perp\frac{|J_{N,N'}(u)|^2}{q_\perp}\\&\times\{[f_{N+1,n}(1-f_{N',n'})-f_{N',n'}(1-f_{N+1,n})]\delta(\varepsilon_{1P})\\&+[f_{N+1,n}(1-f_{N',n'})-f_{N',n'}(1-f_{N+1,n})]\delta(\varepsilon_{1P})\}\\&+\frac{\kappa^2e^2k_bT}{8\hbar L_z\epsilon_s\epsilon_0}\sum_{N'}\sum_{n'}\frac{2+\delta_{n,n'}}{(f_{N+1,n}-f_{N,n})}\int_0^\infty dq_\perp\frac{|J_{N+1,N'}(u)|^2}{q_\perp}\\&\times\{[f_{N',n'}(1-f_{N,n})-f_{N,n}(1-f_{N',n'})]\delta(\varepsilon_{2P})\\&+[f_{N',n'}(1-f_{N,n})-f_{N,n}(1-f_{N',n'})]\delta(\varepsilon_{2P})\},\end{aligned}\quad(34)$$

where

$$\varepsilon_{1P}=(N'-N-1)\hbar\omega_c+\hbar\omega+(n'^2-n^2)\varepsilon_0,\quad(35)$$

$$\varepsilon_{2P}=(N-N')\hbar\omega_c+\hbar\omega+(n^2-n'^2)\varepsilon_0,\quad(36)$$

and the Dirac delta functions, $\delta(\varepsilon_{iP})$, in which ($i=1$, 2) in Eq. (34) are replaced by Lorentzian-width $\gamma_{NN'}$ when $i=1$ and $\gamma_{N+1,N'}$ when $i=2$ as below [33]

$$\delta(\varepsilon_{1P})=\frac{1}{\pi}\frac{\gamma_{NN'}^P}{(\varepsilon_{1P})^2+(\gamma_{NN'}^P)^2},\quad(37)$$

$$\delta(\varepsilon_{2P})=\frac{1}{\pi}\frac{\gamma_{N+1,N'}^P}{(\varepsilon_{2P})^2+(\gamma_{N+1,N'}^P)^2},\quad(38)$$

with

$$\gamma_{N'N}^P=\sqrt{\frac{\kappa^2e^2k_bT}{8\pi L_z\epsilon_s\epsilon_0}(2+\delta_{n,n'})\int_0^\infty dq_\perp\frac{|J_{N,N'}(u)|^2}{q_\perp}},\quad(39)$$

$$\gamma_{N+1,N'}^P=\sqrt{\frac{\kappa^2e^2k_bT}{8\pi L_z\epsilon_s\epsilon_0}(2+\delta_{n,n'})\int_0^\infty dq_\perp\frac{|J_{N+1,N'}(u)|^2}{q_\perp}}.\quad(40)$$

3.2.2. For optical phonon scattering mechanism

In the case of electron-scattering with optical-phonon, the linewidth function for magneto-optical transition $\chi_\gamma(\omega)$ in Eq. (32) is obtained as below [16]

$$\begin{aligned}\chi_\gamma(\omega)\equiv\chi_\gamma^O(\omega)=&\frac{e^2\hbar\omega_0}{8\hbar\epsilon_0L_z}\left[\frac{1}{\epsilon_\infty}-\frac{1}{\epsilon_s}\right]\sum_{N'}\sum_{n'}\frac{2+\delta_{n,n'}}{(f_{N+1,n}-f_{N,n})}\int_0^\infty dq_\perp\frac{|J_{N,N'}(u)|^2}{q_\perp}\\&\times\{[(1+N_q)f_{N+1,n}(1-f_{N',n'})-N_qf_{N',n'}(1-f_{N+1,n})]\delta(\varepsilon_{1O}^-)\\&+[N_qf_{N+1,n}(1-f_{N',n'})-(1+N_q)f_{N',n'}(1-f_{N+1,n})]\delta(\varepsilon_{1O}^+)\}\\&+\frac{e^2\hbar\omega_0}{8\hbar\epsilon_0L_z}\left[\frac{1}{\epsilon_\infty}-\frac{1}{\epsilon_s}\right]\sum_{N'}\sum_{n'}\frac{2+\delta_{n,n'}}{(f_{N+1,n}-f_{N,n})}\int_0^\infty dq_\perp\frac{|J_{N+1,N'}(u)|^2}{q_\perp}\\&\times\{[(1+N_q)f_{N',n'}(1-f_{N,n})-N_qf_{N,n}(1-f_{N',n'})]\delta(\varepsilon_{2O}^-)\\&+[N_qf_{N',n'}(1-f_{N,n})-(1+N_q)f_{N,n}(1-f_{N',n'})]\delta(\varepsilon_{2O}^+)\},\end{aligned}\quad(41)$$

where

$$\varepsilon_{1O}^\pm=(N'-N-1)\hbar\omega_c+\hbar\omega+(n'^2-n^2)\varepsilon_0\pm\hbar\omega_0,\quad(42)$$

$$\varepsilon_{2O}^\pm=(N-N')\hbar\omega_c+\hbar\omega+(n^2-n'^2)\varepsilon_0\pm\hbar\omega_0,\quad(43)$$

and the Dirac delta functions, $\delta(\varepsilon_{iO}^\pm)$ in Eq. (41) are replaced by Lorentzians of width $\gamma_{NN'}^\pm$ for the case of $i=1$ and $\gamma_{N+1,N'}^\pm$ for the case of $i=2$, respectively, as below [33]

$$\delta(\varepsilon_{1O}^\pm)=\frac{1}{\pi}\frac{\gamma_{NN'}^{\pm O}}{(\varepsilon_{1O}^\pm)^2+(\gamma_{NN'}^{\pm O})^2},\quad(44)$$

$$\delta(\varepsilon_{2O}^\pm)=\frac{1}{\pi}\frac{\gamma_{N+1,N'}^{\pm O}}{(\varepsilon_{2O}^\pm)^2+(\gamma_{N+1,N'}^{\pm O})^2},\quad(45)$$

with

$$\gamma_{N'N}^{\pm O}=\frac{e}{2\pi}\sqrt{\frac{\hbar\omega_0}{2\epsilon_0}\left[\frac{1}{\epsilon_\infty}-\frac{1}{\epsilon_s}\right]\left(N_{\mathbf{q}}+\frac{1}{2}\pm\frac{1}{2}\right)M_{nn'}\int_0^\infty dq_\perp\frac{|J_{N,N'}(u)|^2}{q_\perp}},\quad(46)$$

$$\gamma^{\pm O}_{N+1,N'} = \frac{e}{2\pi}\sqrt{\frac{\hbar\omega_0}{2\epsilon_0}\left[\frac{1}{\epsilon_\infty}-\frac{1}{\epsilon_s}\right]}\left(N_{\mathbf{q}}+\frac{1}{2}\pm\frac{1}{2}\right)M_{nn'}\int_0^\infty dq_\perp\frac{|J_{N+1,N'}(u)|^2}{q_\perp}. \quad (47)$$

Based on these calculations we using the profile method to examine the influence of piezoelectric phonons on the magneto-optical transition linewidths by comparing with that due to optical phonons. Obtained results are shown in following section.

4. Numerical calculations for both GaN and GaAs materials and discussions

In this Sec., we show numerical calculated results for MO-transition linewidths of cyclotron-resonance peaks caused by piezoelectric phonons scattering in comparison with that due to the optical-phonons scattering in both GaN and GaAs materials of a square potential quantum well with parameters utilized as [34–38]: $m^* = 0.22 \times m_0$, $\epsilon_0 = 8.85 \times 10^{-12}$ C^2/Nm^2, $\epsilon_s = 9.2$, $\epsilon_\infty = 5.35$, $\hbar\omega_0 = 91.8$ meV, and $\kappa = 2.6 \times 10^{-2}$ m/s for GaN material; $m^* = 0.067m_0$ in which m_0 is the free electron mass, $\epsilon_s = 13.18$, $\epsilon_\infty = 10.89$, $\hbar\omega_0 = 36.25$ meV, and $\kappa = 0.6 \times 10^{-2}$ m/s for GaAs material. Here $E_0 = 5.0 \times 10^6$ V/m. Note that the results were examined in the quantum limit. The electrons occupy $n = 1$, $n' = 1$, 2 and $N = 0$, $N' = 1$ levels are assumed. From the analytical expression for the MOAP in GaAs and GaN quantum-wells caused by electrons scattering effects of piezoelectric and optical phonons. We carry out numerical calculations and plot graphically the photon energy dependence on the MOAP, we find the cyclotron resonance peaks in GaN and GaAs, respectively, as shown in Fig. 1 below.

Fig. 1 describes the photon energy dependence of the magneto-optical absorption power at cyclotron resonance peak due to piezoelectric and optical phonon scattering mechanisms in both GaN (Fig. 1a)) and GaAs (Fig. 1b)), is plotted at $L_z = 10$ nm, $T = 300$ K, $n_e = 1 \times 10^{18}$ cm^{-3}, and the magnetic field $B = 10$ T. Based on the computational method, the positon of resonance peaks are determine to be at the values of photon energies $\hbar\omega = 5.26$ meV and $= 17.29$ meV for GaN and GaAs, respectively. They together satisfy the condition $\hbar\omega = (N' - N)\hbar\omega_c$, namely $5.26 = (1 - 0)5.26$ for GaN and $17.29 = (1 - 0)17.29$ for GaAs. Therefore they referred to as the cyclotron resonance (CR) peaks. These peaks describe the transitions between two Landau-levels: the initial level ($N = 0$) to the final level ($N' = 1$) by $\hbar\omega$-photon-energy absorption. From the graphs which describe photon-energy dependence of the MOAP, we measure the MOTLW of the CR peak, simultaneously determine the variation of the MOTLW with the well width, the electron density, the temperature, and the magnetic field under all piezoelectric and optical phonon scattering mechanisms in GaN and GaAs. Our obtained results as shown in following figures:

Figs. 2 and 3 show that the MOTLWs in GaAs and GaN increase as the temperature and the magnetic field increase for the piezoelectric and optical phonon scattering mechanisms. This implies that the electron scattering strengths of piezoelectric and optical phonons in both GaAs and GaN increase with the increasing temperatures and magnetic fields. We can explain that these rises as being mainly due to the distribution of phonon, i.e., as the temperatures increase, the number of phonon modes participating in the interaction rises and therefore the line-broadening rises with the temperatures. The result also interprets the resonance phenomena in the electrophonon interaction system due to the collision effect of phonon modes caused by the thermal crystal lattice vibration which is expected that it will become larger when the temperatures increase. Furthermore, this is due to the electron scattering possibilities of piezoelectric and optical phonons increase as the temperature and the magnetic field increase under all GaN and GaAs. Besides, it can be explained further that the electron scattering possibilities of piezoelectric and optical phonons increase as the magnetic field increase to be due to the increase of B leads to the rise of electron confinement strength because of the increase of the cyclotron resonance frequency, $\omega_c = eB/m^*$, and the decrease of the cyclotron radius $a_c = \sqrt{\hbar c/(eB)}$. Result is obtained to be qualitative consistent with calculations in experiment by Refs. [39–46]. In particular, our result also shows that the MOTLWs due to electron–piezoelectric phonon scattering vary faster, sharper, and have larger value than they do due to electron–optical-phonons scattering for both GaN and GaAs materials. This is due to the activation of phonon modes rises as the temperature increases. In other words, the electron scattering caused by piezoelectric potential phonon modes with large wave vector rises with the increase of the temperatures. It should be noted that this tendency is different for optical phonon modes

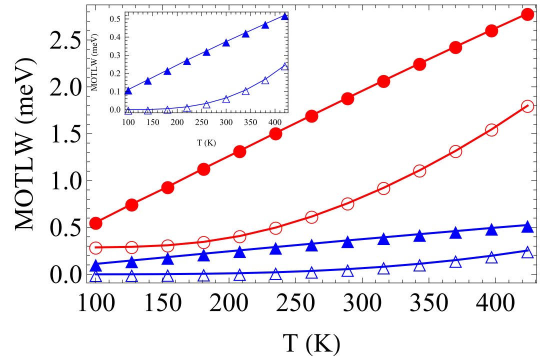

Fig. 2. Influence of the changes in temperature on the MOTLWs due to the piezoelectric- and optical-phonon scattering mechanisms in both GaN and GaAs. Here, the well width $L_z = 10$ nm, the electron density $n_e = 1 \times 10^{18}$ cm^{-3}, and the magnetic field $B = 10$ T. Where the filled-circles and empty-circles curves respectively correspond to the piezoelectric and optical phonons in GaN, the filled-triangles and empty-triangles curves respectively correspond to the piezoelectric and optical phonons in GaAs.

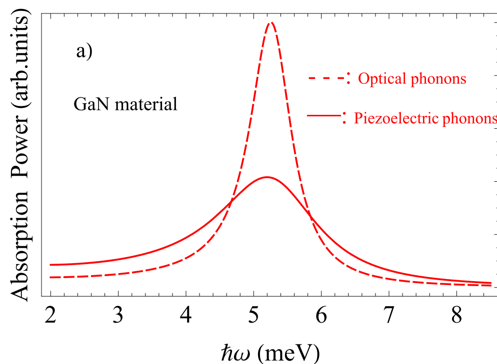

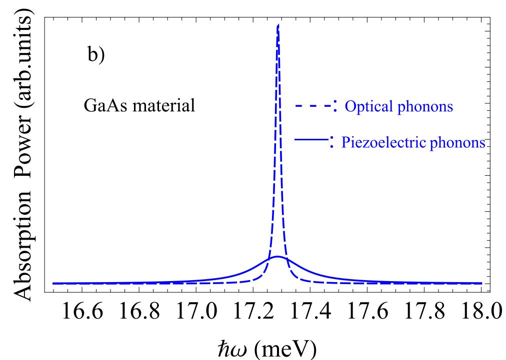

Fig. 1. Magneto-optical absorption power due to piezoelectric and optical phonon scattering mechanisms in GaN and GaAs. Where the well width $L_z = 10$ nm, the temperature $T = 300$ K, electron density $n_e = 1 \times 10^{18}$ cm^{-3}, and the magnetic-field $B = 10$ T.

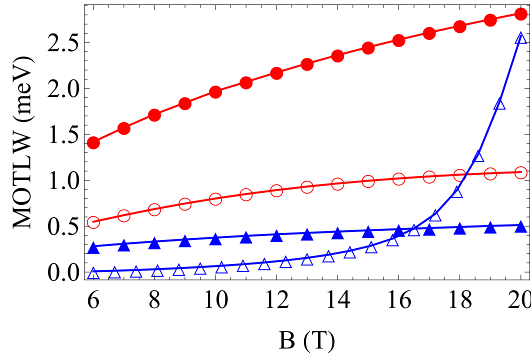

Fig. 3. Influence of the changes in B on the MOTLWs due to the piezoelectric- and optical-phonon scattering mechanisms in both GaN and GaAs. Here, the well width $L_z = 10$ nm, the temperature $T = 300$ K, and the density of the electron $n_e = 1 \times 10^{18}$ cm^{-3}. Where the filled-circles and empty-circles curves respectively correspond to the piezoelectric and optical phonons in GaN, the filled- and empty-triangles curves respectively correspond to the piezoelectric and optical phonons in GaAs.

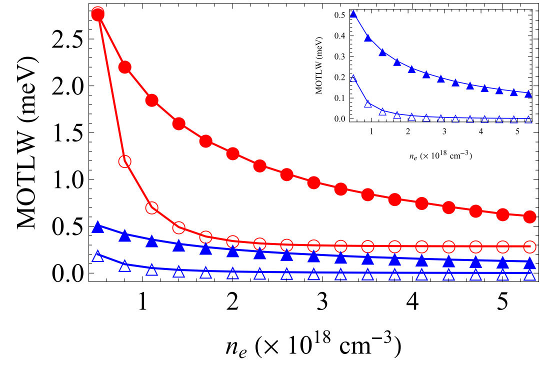

Fig. 4. Influence of the changes in electron density on the MOTLWs due to the piezoelectric- and optical-phonon scattering mechanisms in both GaN and GaAs. Here, the quantum-well width $L_z = 10$ nm, the temperature $T = 300$ K, and the magnetic field $B = 10$ T. Where the filled- and empty-circles curves respectively correspond to the piezoelectric and optical phonons in GaN, the filled- and empty-triangles curves respectively correspond to the piezoelectric and optical phonons in GaAs.

because of optical phonon modes is fair different from piezoelectric potential phonon modes, as shown in the interaction matrix element in Eq. (5) with the coupling-coefficient V_q is given by Eq. (8) for piezoelectric potential phonons and Eq. (16) for optical phonons. Moreover, we also see that the MOTLWs of GaN are larger than those of GaAs for both piezoelectric and optical phonon scattering mechanisms because the piezoelectric coupling constant κ and the optical phonon energy $\hbar\omega_0$ for GaN material ($= 2.6 \times 10^{-2}$ m/s and $= 91.8$ meV) are larger than those for GaAs material ($= 0.6 \times 10^{-2}$ m/s and $= 36.25$ meV), respectively.

In Figs. 4 and 5 are shown in detail the comparisons of the dependence of the electron density and well width on the MOTLWs of both GaN and GaAs due to the piezoelectric and optical phonon scattering mechanisms at the temperature $T = 300$ K, the magnetic-field $B = 10$ T, the quantum-well-width $L_z = 10$ nm and the density of the electron $n_e = 1 \times 10^{18}$ cm^{-3}. From the figures, we see that the MOTLWs are shown to decrease as the well width and the electron density increase for both the piezoelectric and optical phonons in both GaN and GaAs. This result implies that the increasings the quantum-well width and the density of the electron lead to the decreasing the electron scattering strengths of piezoelectric and optical phonons in both GaAs and GaN. It is because the electron scattering possibilities of piezoelectric and optical phonons in all GaN and GaAs decease as the quantum-well-width increases, since the increasing the quantum-well-width leads to the decreasing the electron confinement strength. Result is obtained to be qualitative consistent with calculations in experiment by Refs. [39,42,46–48]. On the other hand, the screening is the cause leads to the decreasing the MOTLWs as the density of the electron increases, as shown in Fig. 4. This property is explained as follows: With the rise of n_e leads to the reciprocal of the Debye screening length $q_d^2 = n_e e^2/\epsilon_s \epsilon_0 k_B T$ increases, and therefore the coupling coefficient V_q in Eqs. (8) and (16) decreases, i.e., the electron scattering effect reduces as the density of the electron rises under all the piezoelectric- and optical-phonon scattering mechanisms. Note that the distribution from electrons in Eqs. (8) and (16) is nondegenerate to be assumed, and this is a simple approximation in order to include the full dynamic screening, we can emphasize that. Moreover, Figs. 4 and 5 also shown in detail the comparisons of the dependence of the electron density and well width on the MOTLWs for all the four cases. From these figures, we see the MOTLWs for the electrons–piezoelectric-phonons interaction decrease sharply with the quantum-well width and the electron density than they do for the electron–optical one under all the GaN and GaAs. It is because the piezoelectric phonon energy has the wave vector dependence q, while the energy of the optical-phonons is almost constant, i.e., the piezoelectric-phonon mode reduces with the wave vector q, while that is almost invariant for the optical phonon mode. In other words, the quantities with larger wave vector q those contribute more to the electron scattering as the electron density rises, as shown in Eqs. (8) and (16). Fig. 5 also indicates that the important contribution of the piezoelectric phonon to MOTLW and cannot be neglected as small enough quantum-well width.

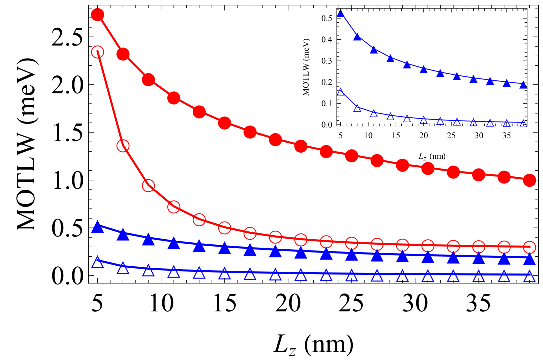

Fig. 5. Influence of the changes in L_z on the MOTLWs due to the piezoelectric- and optical-phonon scattering mechanisms in both GaN and GaAs. Here, the temperature $T = 300$ K, electron density $n_e = 1 \times 10^{18}$ cm^{-3}, and the magnetic field $B = 10$ T. Where the filled-circles and empty-circles curves respectively correspond to the piezoelectric- and optical-phonons in GaN, the filled-triangles and empty-triangles curves respectively correspond to the piezoelectric and optical phonons in GaAs.

5. Conclusions

We have studied the influence of piezoelectric phonons on the magneto-optical transition linewidths compared with optical phonons in both GaAs and GaN materials of a single quantum well. Using the projection operator we have obtained the analytical expressions for the MOCT and the MOAP of the electrons system in well. Through the numerical calculations of the analytical results, we have found the following properties of piezoelectric phonon scattering mechanism in GaN and GaAs compared with optical phonon one as follows: (i) The MOTLWs of GaAs and GaN increase as the magnetic-field and the temperature increase, but decrease as the quantum-well width and electron density increase for both the piezoelectric- and optical-phonon scattering mechanisms. (ii) The MOTLWs caused by electron–piezoelectric

phonon scattering vary sharper, and have larger-value than they do due to electron–optical-phonon scattering in both GaN and GaAs materials of the quantum well. (iii) The MOTLWs of GaN are larger than those of GaAs for both piezoelectric and optical phonon scattering mechanisms. (iv) The contribution of the piezoelectric phonons to the MOTLWs is significant and more dominant than that of the optical phonons in both GaN and GaAs. (v) The influence of piezoelectric phonons on the magneto-optical transition linewidths compared with optical phonons in both GaN and GaAs materials of a single quantum well is considerable and cannot be neglected as the width of the quantum-well is small enough. We expect that the results of this detailed theoretical study will help to analyze experimentally the electron–piezoelectric potential phonon scattering mechanism in the materials.

Declaration of competing interest

We declare that we have no significant competing financial, professional, or personal interests that might have influenced the performance or presentation of the work described in this manuscript.

References

[1] N.D. Hien, C.V. Nguyen, N.N. Hieu, S.S. Kubakaddi, C.A. Duque, M.E. Mora-Ramos, L. Dinh, T.N. Bich, H.V. Phuc, Phys. Rev. B 101 (2020), 045424.
[2] P. Vasilopoulos, Phys. Rev. B 33 (1986) 8587–8594.
[3] N.L. Kang, J.Y. Ryu, S.D. Choi, J. Phys. Condens. Matter 14 (41) (2002) 9733–9742.
[4] N. Lyong Kang, S. Don Choi, J. Phys. Soc. Jpn. 78 (2) (2009), 024710.
[5] S.Y. Choi, S.C. Lee, H.J. Lee, H.S. Ahn, S.W. Kim, J.Y. Ryu, Phys. Rev. B 66 (2002), 155208.
[6] G.-Q. Hai, F.M. Peeters, Phys. Rev. B 60 (1999) 16513–16518.
[7] C. Chen, M. Dutta, M.A. Stroscio, J. Appl. Phys. 95 (5) (2004) 2540–2546.
[8] J.-j. Shi, Phys. Rev. B 68 (2003), 165335.
[9] S. Tanaka, Y. Honda, N. Sawaki, M. Hibino, Appl. Phys. Lett. 79 (7) (2001) 955–957.
[10] Y. Honda, Y. Kuroiwa, M. Yamaguchi, N. Sawaki, Appl. Phys. Lett. 80 (2) (2002) 222–224.
[11] N.D. Vy, L.N. Minh, N.T. Tuyet Anh, H.D. Trien, N.D. Hien, Superlattice. Microst. 145 (2020), 106626.
[12] N.D. Hien, Optik 206 (2020), 164348.
[13] H.K. Dan, L. Dinh, H.D. Trien, T.C. Phong, N.D. Hien, Phys. E Low-dimens. Syst. Nanostruct. 120 (2020), 114043.
[14] K. Doan Quoc, H. Nguyen Dinh, Opt. Quant. Electron. 51 (4) (2019) 116.
[15] L.T.T. Phuong, L. Dinh, N.D. Hien, J. Phys. Chem. Solid. 136 (2020), 109127.
[16] N.D. Hien, Phys. E Low-dimens. Syst. Nanostruct. 114 (2019), 113608.
[17] N.D. Hien, L. Dinh, N.T. Tuyet Anh, J. Phys. Chem. Solid. 145 (2020), 109501.
[18] P.N. Argyres, J.L. Sigel, Phys. Rev. B 10 (1974) 1139–1148.
[19] A. Suzuki, D. Dunn, Phys. Rev. B 25 (1982) 7754–7764.
[20] N.D. Hien, Superlattice. Microst. 131 (2019) 86–94.
[21] N.D. Hien, C. Duque, E. Feddi, N.V. Hieu, H.D. Trien, L.T. Phuong, B.D. Hoi, L. T. Hoa, C.V. Nguyen, N.N. Hieu, H.V. Phuc, Thin Solid Films 682 (2019) 10–17.
[22] T.C. Phong, L.T.T. Phuong, N.D. Hien, V.T. Lam, Phys. E Low-dimens. Syst. Nanostruct. 71 (2015) 79–83.
[23] J.S. Bhat, S.S. Kubakaddi, B.G. Mulimani, J. Appl. Phys. 70 (4) (1991) 2216–2219.
[24] Y.J. Cho, S.D. Choi, Phys. Rev. B 49 (1994) 14301–14306.
[25] N. Kang, Y. Ji, H.J. Lee, S. Choi, J. Kor. Phys. Soc. 42 (2003) 379–385.
[26] N. Kang, Y. Lee, S. Choi, J. Kor. Phys. Soc. 44 (2004) 1535–1541.
[27] P. Vasilopoulos, Phys. Rev. B 33 (1986) 8587–8594.
[28] G.-Q. Hai, F.M. Peeters, Phys. Rev. B 60 (1999) 8984–8991.
[29] A.R. Hutson, J. Appl. Phys. 32 (10) (1961) 2287–2292.
[30] D.K. Ferry, Semiconductors, Macmillan Publishing Co., New York, 1991.
[31] J.Y. Sug, S.G. Jo, J. Kim, J.H. Lee, S.D. Choi, Phys. Rev. B 64 (2001), 235210.
[32] N. Lyong Kang, J.H. Lee, D.-S. Choi, J. Kor. Phys. Soc. 37 (2000) 339–342.
[33] M.P. Chaubey, C.M. Van Vliet, Phys. Rev. B 33 (1986) 5617–5622.
[34] J.S. Bhat, B.G. Mulimani, S.S. Kubakaddi, Phys. Rev. B 49 (1994) 16459–16466.
[35] S. Adachi, J. Appl. Phys. 58 (3) (1985) R1–R29.
[36] J. Gong, X.X. Liang, S.L. Ban, J. Appl. Phys. 100 (2) (2006), 023707.
[37] S.H. Lee, J.Y. Sug, J.Y. Choi, G. Sa-Gong, J.T. Lee, in: 2009 IEEE International Ultrasonics Symposium, 2009, pp. 1620–1623.
[38] J.Y. Sug, S.H. Lee, J. Nanosci. Nanotechnol. 18 (10) (2018).
[39] M. Singh, Phys. Rev. B 35 (1987) 9301–9304.
[40] T. Unuma, T. Takahashi, T. Noda, M. Yoshita, H. Sakaki, M. Baba, H. Akiyama, Appl. Phys. Lett. 78 (22) (2001) 3448–3450.
[41] P. von Allmen, M. Berz, G. Petrocelli, F.K. Reinhart, G. Harbeke, Semicond. Sci. Technol. 3 (12) (1988) 1211–1216.
[42] T. Unuma, M. Yoshita, T. Noda, H. Sakaki, H. Akiyama, J. Appl. Phys. 93 (3) (2003) 1586–1597.
[43] P. Voisin, Y. Guldner, J.P. Vieren, M. Voos, P. Delescluse, N.T. Linh, Appl. Phys. Lett. 39 (12) (1981) 982–984.
[44] K. Muro, S. Mori, S. Narita, S. Hiyamizu, K. Nanbu, Surf. Sci. 142 (1) (1984) 394–399.
[45] B. Tanatar, M. Singh, Phys. Rev. B 43 (1991) 6612–6619.
[46] N. Holonyak, R.M. Kolbas, W.D. Laidig, M. Altarelli, R.D. Dupuis, P.D. Dapkus, Appl. Phys. Lett. 34 (8) (1979) 502–505.
[47] K.L. Campman, H. Schmidt, A. Imamoglu, A.C. Gossard, Appl. Phys. Lett. 69 (17) (1996) 2554–2556.
[48] M. Belmoubarik, K. Ohtani, H. Ohno, Appl. Phys. Lett. 92 (19) (2008), 191906.